Optics Letters

Fano-resonance-based mode-matching hybrid metasurface for enhanced second-harmonic generation

Zhi Li, Wenwei Liu, Zhancheng Li, Hua Cheng, Shuqi Chen,* and Jianguo Tian

Key Laboratory of Weak Light Nonlinear Photonics, Ministry of Education, School of Physics and TEDA Institute of Applied Physics, Nankai University, Tianjin 300071, China
**Corresponding author: schen@nankai.edu.cn*

Received 28 June 2017; revised 13 July 2017; accepted 14 July 2017; posted 14 July 2017 (Doc. ID 301177); published 8 August 2017

Plasmonic nanostructures have been considered as potential candidates for enhancing the nonlinear upconversion rate at nanoscale levels due to their strong near-field enhancement. Here, we propose a Fano-resonance-based mode-matching hybrid metasurface that combines the advantages of Fano resonances and mode-matching for boosting second-harmonic conversion. A confined and strong near-field intensity is generated by gold nanoantennas within the volume of polycrystalline zinc sulfide nanoparticles, thus resulting in a larger effective second-harmonic coefficient. The combination of the abovementioned features allows for the realization of a second-harmonic generation (SHG) conversion efficiency of 5.55×10^{-8}, and the SHG signal is twice that obtained with dipole hybrid metasurfaces. Our designed metasurface may pave the way for optimizing nonlinear light-matter interactions at the nanoscale.

OCIS codes: (160.3918) Metamaterials; (190.2620) Harmonic generation and mixing; (190.4390) Nonlinear optics, integrated optics.

https://doi.org/10.1364/OL.42.003117

Second-harmonic generation (SHG) is a process in nonlinear optics wherein two photons at the same frequency are converted into one photon with double this frequency, and it has been applied extensively in lasers, the measurement of ultrashort-width pulses, morphology detection of metal nanoobjects, and medical imagings [1–3]. Owing to the intrinsically weak optical response of nonlinear materials, efficient conversion requires a "long" material interaction length or strong field intensity. Although the process can be distinctly enhanced by satisfying phase-matching conditions, a long light-matter interaction length is still required that is not generally possible with nanoscale integrated optical devices. One strategy to overcome this problem is to employ plasmonic nanostructures, which have the unique ability to localize electromagnetic fields in nanoscale volumes far beyond the diffraction limit while also permitting control of the properties of incident light at dimensions significantly smaller than its wavelength [4]. Hybrid nanostructures, which compose a plasmonic part for enhancement of the electric field and another material for generation of efficient SHG, have been proposed for an even stronger nonlinear conversion [5,6]. Moreover, such plasmonic devices afford great design flexibility since nanostructures do not require phase-matching. In this context, mode-matching has been found as another efficient approach to improve upconversion efficiency [7,8]. When the nanostructure is in resonance with the incoming radiation, the field enhancement effect of the fundamental field amplifies the upconversion. Meanwhile, the generated nonlinear signal can be efficiently radiated to the far-field by the nanostructure, which is resonant with respect to the nonlinear field [9]. This effective combination of the plasmonic multiresonance and the spatial overlap of the involved plasmonic modes significantly enhances the nonlinearity.

Plasmonic Fano resonances arising from interference of bright super-radiant and dark subradiant modes in nanostructures have found applications in physical, chemical, and biological sciences [10–12]. The narrow dip in the scattering spectrum of a Fano-resonant plasmonic system results in the suppression of radiative losses and strong near-field enhancement, making Fano resonances particularly efficient for boosting nonlinear conversion. For this reason, researchers have aimed at enhancing the nonlinear response of optical materials with Fano-resonant nanostructures in recent years [13–15]. Although such approaches have effectively increased nonlinear conversion, the designed nanostructures have thus far exploited only the aspects of reducing radiation losses or confining electromagnetic fields. On the other hand, efficient SHG emission cannot be achieved with such approaches since traditional Fano-resonant nanostructures are usually fabricated with noble metals, whose centrosymmetric atomic lattice forbids SHG in the bulk of these metals as per the electric dipole approximation.

In this Letter, we proposed a hybrid metasurface that combines mode-matching with Fano resonances. Consequently, the SHG benefits from the doubly resonant nanostructure with spatial-mode overlap at both the fundamental and second-harmonic wavelengths; meanwhile, via engineering of the Fano resonance at the SHG wavelength, the gold nanoantennas

act as an efficient receiving optical system, thereby providing suitable field enhancement and satisfying the SHG emission conditions for SHG conversion. Furthermore, polycrystalline zinc sulfide (ZnS) nanoparticles with noncentrosymmetric unit patterns located at the gaps of the nanoantennas act as even stronger SHG converters. The designed metasurface results in a conversion efficiency on the order of 10^{-8} with a peak pump intensity of 3.2 GW $\cdot$ cm^{-2}. In addition, we compare the SHG response of our doubly resonant metasurface to resonance only at the fundamental wavelength, thus demonstrating that the use of Fano resonance at the SHG wavelength effectively enhances the SHG conversion. The proposed metasurface can pave the way for the applications of Fano resonances and mode-matching in nonlinear optics.

In regards to the first theoretical prediction and experimental realization of Fano resonances in nanostructures in the optical regime, researchers have previously reported on a nonconcentric ring-disk cavity that allows coupling between a narrow quadrupolar ring mode and a broad dipolar disk mode, resulting in a pronounced quadrupolar Fano resonance [16]. Subsequently, the generation of higher-order, stronger Fano resonances has also been demonstrated with the use of this classic nanostructure [17,18]. To achieve stronger, higher-order Fano resonances, here, we employ a dual-disk ring (DDR) nanostructure, which has been shown to suppress quadrupolar resonance while enhancing the octupolar Fano resonance. Figure 1 illustrates the hybrid metasurface in which the ZnS nanoparticles (in pink) are enclosed by patterned gold DDR Fano systems. The metasurface is characterized by five geometrical parameters: inner and outer radii r_i and r_o of the ring, radius a of the two disks, nanogap g between the ring and each disk, and thickness h of the gold layer. The ZnS nanoparticles (also with thickness h) are located in the gaps between the two disks in each unit cell, and, meanwhile, their sizes are chosen to ensure that they just contact the gold disks. The incident electric field lies along the x axis, which is parallel to the plane of the gold nanodisks. In our study, all numerical simulations were performed with the use of the finite-difference time-domain (FDTD) approach based on the commercial software package, Lumerical Solutions [19]. A single meta-atom was actually simulated by setting perfectly matched layers in all the simulated direction. The solver-defined total-field scattered-field (TFSF) formulation was performed, and the scattering cross-section (SCS) was calculated from the sum of the power flowing outward through a volume enclosing the TFSF source. The complex dielectric constants of gold were taken from measured data [20], and the refractive index of ZnS and silica substrate was taken as 2.27 and 1.5, respectively.

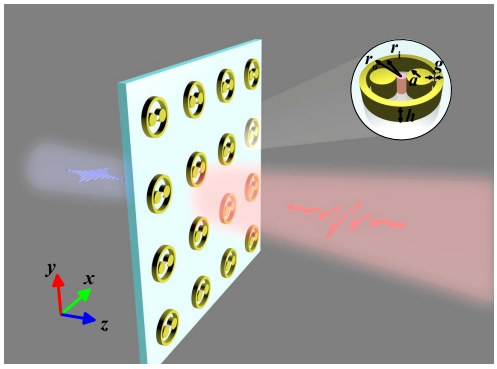

Fig. 1. Schematic of two-photon upconversion with the proposed hybrid metasurface. The inset shows a unit cell of the metasurface with geometrical parameters of $r_i = 105$ nm, $r_o = 125$ nm, $a = 40$ nm, $g = 10$ nm, and $h = 60$ nm.

To satisfy the mode-matching condition, the resonances of the plasmonic system need to be specifically optimized at both the fundamental and SHG wavelengths. Figure 2(a) shows the SCS of the hybrid metasurface and the near-field enhancement at the center of the ZnS nanoparticles. Dipolar resonance occurs at the fundamental wavelength, and the enhanced octupolar Fano resonance is simultaneously tuned to match the SHG emission wavelength. The actual position of Fano resonances has been proved to be related to the near-field enhancement by the subradiant mode [21]. As a consequence, the Fano resonance of the hybrid metasurface exhibits a slight redshift with respect to the Fano dip, and it lies closer to the Fano peak of the scattering spectrum, indicating that the octupolar Fano resonance contributes to both SHG wavelength emission and strong field enhancement. To verify the properties of the resonances at the fundamental and SHG wavelengths, we further calculated the corresponding charge distributions and near-field intensities. Figures 2(b) and 2(c) depict the charge distributions relative to the main resonances of the metasurface at wavelengths of 750 nm and 1500 nm, respectively. From Fig. 2(b), we note that there are six nodes on the ring, corresponding to the enhanced octupolar Fano resonance by using the symmetric dual-disk. The charge distribution on the ring exhibits only two nodes representing dipolar resonance, as shown in Fig. 2(c). The simulated field enhancements of the ZnS nanoparticles at wavelengths of 750 nm and 1500 nm are shown in Figs. 2(d) and 2(e), respectively, and interestingly, they are of the same order as those of advanced nonlinear plasmonic devices [7,8]. In comparison to the field enhancement of their

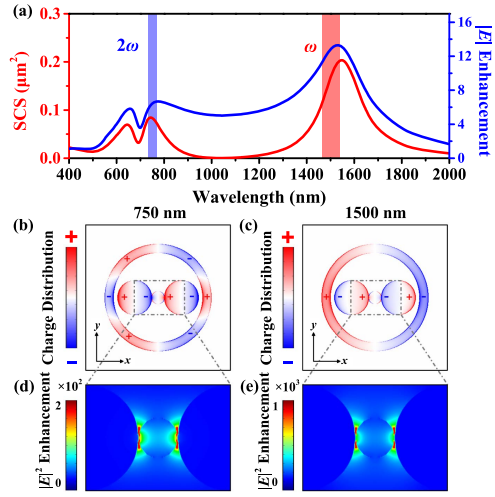

Fig. 2. (a) Scattering cross-section (red line) of the hybrid metasurface and the near-field enhancement (blue line) at the center of ZnS nanoparticles. The spectrum shows a simultaneous pronounced overlap with the fundamental and SHG wavelengths, which are marked by red and blue stripes. (b) and (c) Charge distributions relative to the main resonances of the metasurface at wavelengths of 750 nm and 1500 nm. (d) and (e) Near-field enhancements of ZnS nanoparticles at wavelengths of 750 nm and 1500 nm.

noble-metal counterparts, here, field enhancement occurs within the volume of ZnS nanoparticles, resulting in a larger effective SHG coefficient.

To evaluate the enhancement independently of the ZnS nanoparticles, we calculated the SHG enhancement factor τ, which is defined as the ratio of the SHG intensity converted from the metasurface to that of the ZnS nanoparticles. We began our nonlinear investigations by simulating the SHG from the hybrid metasurface. Although the contributions of surface susceptibilities are larger than the bulk term (especially $\chi^{(2)}_{\perp\perp\perp}$), they still behave "like bulk" when induced by the fast field variation at the metal interface [4]. Therefore, the effective bulk susceptibility 0.78 pm $\cdot$ V^{-1} is used to simulate the SHG emission in gold [22]. And the isotropic second-order susceptibility of polycrystalline ZnS was 2 pm $\cdot$ V^{-1} [9]. In the simulation, the metasurface was illuminated with a normal-incident Gaussian pulse with a field amplitude of 1.55×10^8 V $\cdot$ m^{-1}, corresponding to a peak field intensity of 3.2 GW $\cdot$ cm^{-2}, which is less than the damage threshold of gold [23]. A narrowband Gaussian pulse with initial time delay of 400 fs and the full width at half-maximum of 150 fs is incident on the designed structure, corresponding to spectral width of 22.05 nm after Fourier transform. Figure 3(a) illustrates the SHG enhancement factor τ for the hybrid metasurface (blue line). The red-dashed line represents the ratio of the pump light to the SHG from ZnS nanoparticles. The fundamental femtosecond excitation at 1500 nm yields the instantaneous SHG response centered at 750 nm, as shown in Fig. 3(b) depicting the magnified SHG response at around 750 nm. Upon defining the SHG conversion efficiency as $\eta_{SH} = P_{SH}/P_{FF}$ (where $P_{FF} = I_{FF} \cdot A$ represents the power at the fundamental wavelength, I_{FF} the pump intensity, and A the unit cell area) [24], we calculated the conversion efficiency to be 5.55×10^{-8}. To quantitatively determine the nonlinear enhancement of the hybrid metasurface, we compared the SHG response of the bare gold nanoantennas and isolated ZnS nanoparticles (of identical thickness) to that of the hybrid metasurface, as shown in Figs. 3(b) and 3(c). Our results indicate that the intrinsic SHG background of the bare nanoantennas is much smaller than that of the hybrid metasurface due to its centrosymmetric structure. The third-harmonic generation signal is mainly contributed by dielectric when its susceptibility is comparable to or higher than gold [25]. To distinguish the main contribution of the SHG signal, we simulated the conversion efficiency for different hybrid nanostructures: (1) the conversion efficiency is 5.55×10^{-8} for the emission from the hybrid nanostructure ($\chi_{Au}(2) \neq 0$ and $\chi_{ZnS}(2) \neq 0$); (2) the conversion efficiency is 5.55×10^{-8} for the emission only from ZnS nanoparticle ($\chi_{Au}(2) = 0$ and $\chi_{ZnS}(2) \neq 0$); and (3) the conversion efficiency is 1.81×10^{-12} for the emission only from gold DDR nanostructure ($\chi_{Au}(2) \neq 0$ and $\chi_{ZnS}(2) = 0$). These results confirm that the main contribution of the SHG is from the ZnS nanoparticle. Such a large enhancement in the SHG signal primarily results from the Fano-resonance-based mode-matching condition satisfied by the plasmonic DDR nanostructures.

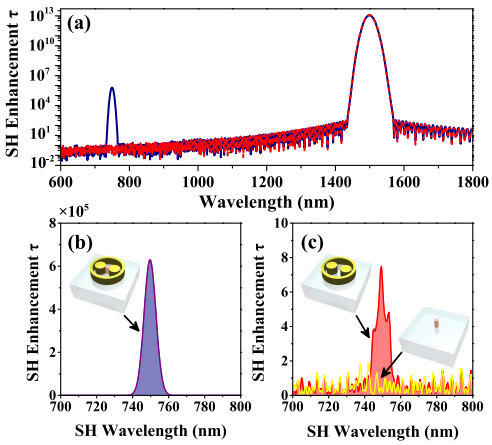

Fig. 3. (a) Log plot of the spectrum of SHG response (blue line) as defined by the SHG enhancement factor τ. The red-dashed line represents the pump light with the same processing. (b) Magnified view of the SHG spectrum centered at 750 nm. The inset shows a unit of the hybrid metasurface. (c) SHG spectra of bare gold nanoantennas and isolated ZnS nanoparticles. The insets show a unit of bare gold nanoantennas (left) and isolated ZnS nanoparticle (right).

To investigate the influence of the incident polarization on the SHG intensity, we plot the normalized SHG emission intensity of the hybrid metasurface as a function of the polarization angle for the incident fundamental light in Fig. 4(a). The SHG signal exhibits a strong dependence on the polarization of the incident light, and the largest SHG signal is achieved when the polarization direction of the incident light lies along the x direction with polarization angle $\theta = 0°$. The intensity of the SHG signal gradually decreases as the polarization direction of the incident light points away from the x direction. Finally, the SHG signal becomes zero as the polarization direction of the incident light points along the y direction, with polarization angle $\theta = 90°$. Although enhanced octupolar Fano resonances can also be generated under perpendicular polarization (90°), near-field enhancement does not occur within the ZnS nanoparticles in this case [17]. This results in the hybrid metasurface selectively enhancing the SHG signal along its own axis due to the strong but different Fano resonances. Figure 4(b) depicts the polarization distribution of the radiated SHG signal. As expected, the SHG signal from the hybrid metasurface exhibits a similar polarimetric response to the incident light, exhibiting maximum SHG intensity for parallel polarization (0°) and minimum SHG intensity (close to 0) for perpendicular polarization (90°).

To further illustrate the role of the octupolar Fano resonance at the SHG wavelength, we investigated another hybrid metasurface consisting of dipole antennas and ZnS nanoparticles [Fig. 5(a)] that only exhibits resonance at the fundamental wavelength. These nanoantennas had the following physical

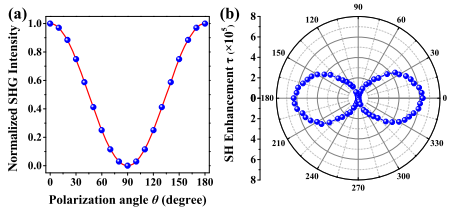

Fig. 4. (a) Normalized SHG emission intensity (blue spheres) and the fitting function $\cos(\theta)^2$ (red line) from the hybrid metasurface under different incident-excitation-light polarizations. (b) Polar diagram of the polarization of the generated SHG signal from the hybrid metasurface.

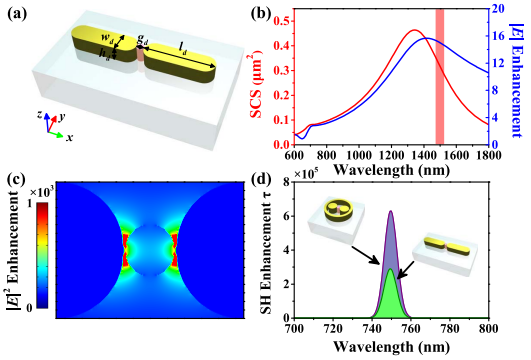

Fig. 5. (a) Sketch of a unit cell of the dipole hybrid metasurface. (b) Scattering cross-section (red line) of the dipole hybrid metasurface and the near-field enhancement (blue line) at the center of ZnS nanoparticles. (c) Near-field enhancement of the ZnS nanoparticle at a wavelength of 1500 nm. (d) Magnified view of the SHG spectra of the Fano-resonance-based hybrid metasurface and the dipole hybrid metasurface as reflected by the SHG enhancement factor τ.

dimensions: length $l_d = 270$ nm, height $h_d = 60$ nm, and gap width $g_d = 30$ nm. The ZnS nanoparticles with identical heights (60 nm) had radii of 15 nm. The width of the nanoantennas was chosen to be $w_d = 80$ nm such that the semicircles at both ends of each nanoantenna had the same radii as those of the disk nanoantennas of the Fano-based hybrid metasurface. Figure 5(b) shows the SCS of the dipole hybrid metasurface and the near-field enhancement at the center of the ZnS nanoparticles. To ensure that there is similar field enhancement for the ZnS nanoparticles, we adjusted the lengths of the nanoantennas, resulting in a blueshift of the resonance peak. Figure 5(c) shows the near-field enhancement of the ZnS nanoparticle at the wavelength of 1500 nm. The SHG enhancement factors τ of the dipole hybrid metasurface and the Fano-resonance-based hybrid metasurface are plotted as a function of the wavelength in Fig. 5(d), and the results indicate that the SHG emission intensity of the Fano-resonance-based hybrid metasurface is more than twice that of the dipole hybrid metasurface. This remarkable enhancement for the Fano-resonance-based hybrid metasurface can be attributed to both SHG wavelength emission and strong field enhancement induced by the presence of octupolar Fano resonance at the SHG wavelength.

In conclusion, we proposed a Fano-resonance-based mode-matching hybrid metasurface comprising gold DDR antennas and ZnS nanoparticles. Our investigations showed that the SHG signal that mainly originated from ZnS nanoparticles benefits from the presence of Fano resonances at the SHG wavelength. As a result, a conversion efficiency of 5.55×10^{-8} with a peak pump intensity of 3.2 GW $\cdot$ cm^{-2} could be achieved with our setup. Moreover, the Fano-resonance-based mode-matching hybrid metasurface provides an SHG enhancement that is more than twice that of the dipole hybrid metasurface, illustrating that the presence of Fano resonance at the SHG wavelength can distinctly enhance SHG conversion. Such a platform can also be applied for other nonlinear processes, including parametric downconversion and difference frequency generation. We believe that our work extends the understanding of the impact of Fano resonance and mode-matching in plasmonic nanostructures, and hence can open new avenues for more effective nonlinear plasmonic devices.

Funding. National Key Research and Development Program of China (2016YFA0301102); National Natural Science Foundation of China (NSFC) (11574163, 61378006).

Acknowledgment. We also acknowledge the support from the Collaborative Innovation Center of Extreme Optics, Shanxi University, Taiyuan, Shanxi 030006, China.

REFERENCES

1. P. A. Franken, A. E. Hill, C. W. Peters, and G. Weinreich, Phys. Rev. Lett. **7**, 118 (1961).
2. R. W. Boyd, *Nonlinear Optics*, 3rd ed. (Academic, 2008).
3. Y. R. Shen, *The Principles of Nonlinear Optics* (Wiley-Interscience, 1984).
4. J. Butet, P.-F. Brevet, and O. J. F. Martin, ACS Nano **9**, 10545 (2015).
5. D. Lehr, J. Reinhold, I. Thiele, H. Hartung, K. Dietrich, C. Menzel, T. Pertsch, E.-B. Kley, and A. Tünnermann, Nano Lett. **15**, 1025 (2015).
6. H. Aouani, M. Rahmani, M. Navarro-Cía, and S. A. Maier, Nat. Nanotechnol. **9**, 290 (2014).
7. M. Celebrano, X. Wu, M. Baselli, S. Großmann, P. Biagioni, A. Locatelli, C. D. Angelis, G. Cerullo, R. Osellame, B. Hecht, L. Duò, F. Ciccacci, and M. Finazzi, Nat. Nanotechnol. **10**, 412 (2015).
8. K. Thyagarajan, S. Rivier, A. Lovera, and O. J. F. Martin, Opt. Express **20**, 12860 (2012).
9. H. Linnenbank, Y. Grynko, J. Förstner, and S. Linden, Light Sci. Appl. **5**, e16013 (2016).
10. A. B. Khanikaev, C. Wu, and G. Shvets, Nanophotonics **2**, 247 (2013).
11. B. Luk'yanchuk, N. I. Zheludev, S. A. Maier, N. J. Halas, P. Nordlander, H. Giessen, and C. T. Chong, Nat. Mater. **9**, 707 (2010).
12. A. E. Miroshnichenko, S. Flach, and Y. S. Kivshar, Rev. Mod. Phys. **82**, 2257 (2010).
13. K. Thyagarajan, J. Butet, and O. J. F. Martin, Nano Lett. **13**, 1847 (2013).
14. Y. Yang, W. Wang, A. Boulesbaa, I. I. Kravchenko, D. P. Briggs, A. Puretzky, D. Geohegan, and J. Valentine, Nano Lett. **15**, 7388 (2015).
15. S.-D. Liu, E. S. P. Leong, G.-C. Li, Y. Hou, J. Deng, J. H. Teng, H. C. Ong, and D. Y. Lei, ACS Nano **10**, 1442 (2016).
16. F. Hao, Y. Sonnefraud, P. V. Dorpe, S. A. Maier, N. J. Halas, and P. Nordlander, Nano Lett. **8**, 3983 (2008).
17. L. Niu, J. B. Zhang, Y. H. Fu, S. Kulkarni, and B. Luk'yanchuk, Opt. Express **19**, 22974 (2011).
18. Y. H. Fu, J. B. Zhang, Y. F. Yu, and B. Luk'yanchuk, ACS Nano **6**, 5130 (2012).
19. FDTD Solutions by Lumerical Solutions, Inc., http://www.lumerical.com/.
20. P. B. Johnson and R. W. Christy, Phys. Rev. B **6**, 4370 (1972).
21. B. Gallinet and O. J. F. Martin, ACS Nano **5**, 8999 (2011).
22. S. Keren-Zur, O. Avayu, L. Michaeli, and T. Ellenbogen, ACS Photon. **3**, 117 (2016).
23. L. Gui, S. Bagheri, N. Strohfeldt, M. Hentschel, C. M. Zgrabik, B. Metzger, H. Linnenbank, E. L. Hu, and H. Giessen, Nano Lett. **16**, 5708 (2016).
24. S. Campione, A. Benz, M. B. Sinclair, F. Capolino, and I. Brener, Appl. Phys. Lett. **104**, 131104 (2014).
25. A. Calà Lesina, P. Berini, and L. Ramunno, Opt. Mater. Express **7**, 001575 (2017).